

PRELIMINARY MEASUREMENTS OF PROTON POLARIZATION
IN HIGH ENERGY INCLUSIVE PROCESSES*

M. D. Corcoran, S. E. Ems, S. W. Gray, B. A. Martin,
H. A. Neal, H. O. Ogren, R. O. Polvado,
D. R. Rust, J. R. Sauer, and P. Smith

Department of Physics
Indiana University
Bloomington, Indiana 47401

Abstract

A preliminary measurement of inclusive proton polarization at $P_T = 1.1$ GeV/c and $x = .89$ has been completed at the internal target area of Fermilab. Measurements were made at 100, 200, 300, 400 GeV beam energies using a carbon target.

*Work supported by U.S. Energy Research and Development Administration under Contract E(11-1)2009, Task A. Paper presented at the American Physical Society Meeting April 26, 1977, Washington, D.C.

INTRODUCTION

The Indiana University experiment E313 at Fermi National Accelerator Laboratory has undertaken an extensive series of measurements of polarization in proton-proton interactions. Most of this work has been devoted to a measurement of recoil polarization in proton-proton elastic collisions using an unpolarized hydrogen jet target. This note reports on data taken during a few days devoted to inclusive proton polarization--Nov. 15, 1976, Feb. 4, 5, 1977, and March 23, 1977.

The study of the inclusive processes is a natural extension of the elastic measurement. As depicted in Figure 1, inclusive final states can be viewed as a massive particle recoiling against the observed proton. In the forward region ($x > .9$) these inclusive cross-sections can in turn be calculated as the square of a triple regge amplitude (Figure 1c). Spin flip and non-flip terms can interfere in this triple regge picture to produce a polarization of the observed proton.

All of the measurements described in this note made use of a rotating carbon target in the accelerating beam of the FNAL proton accelerator at the Internal Target Area - CO. The proton kinematics were determined by the internal target superconducting spectrometer.

INTERNAL TARGET SPECTROMETER-KINEMATIC PARAMETERS

Details of the internal spectrometer (Figure 2) and the polarimeter (Figure 3) have appeared elsewhere,¹ and will not be repeated in this note.

The spectrometer can be remotely positioned in angle and can select particle momenta between $0 \rightarrow 2.5$ GeV/c (momentum acceptance of $\pm 5\%$ at

polarimeter). The inclusive $p + p \rightarrow p + X$ kinematics are depicted in Figures 4a, 4b, and 4c. Selection of the magnet current determines the momentum and therefore the kinetic energy of the identified proton. Thus, each setting corresponds to a fixed four momentum transfer to the proton, $t = -2m_p T$. However, the recoil missing mass selected is a function of the beam energy. As can be seen from Figure 4c at 52° ($t = 1.4 \text{ GeV}^2$, $P_T = 1.4 \text{ GeV}/c$) beam energies from 50 to 400 GeV select missing masses from $M^2 = 20 \text{ (GeV}/c)^2$ to $120 \text{ (GeV}/c)^2$. Since the rotating carbon target is in the accelerating beam, we simply gate on our experiment at 100, 200, 300, 400 GeV with the resulting missing mass samples shown in Figure 5.

POLARIZATION ANALYSIS

Proton events were selected by cuts on the TOF between H_1 and T_1 (Figures 2 and 3). This separation of pions and protons was quite satisfactory for this momentum setting of $1.4 \text{ GeV}/c$. In fact, the total uncut fraction of pions to protons is less than 10%.

Figure 6 shows a sample of left-right scatters measured in the polarimeter with the 2-inch carbon scatterer. The events have already been cut and selected in several ways. Events in the polarimeter could show only one spurious track in either chamber plane (x,y) following the carbon block and they had to project to the correct hodoscope. Events with an additional hodoscope firing were rejected. These stringent requirements were imposed in order to eliminate all multi-track events after the carbon block which could be due to proton interactions in the carbon. Constraints

of ± 2 inches were also placed on the reconstructed scattering vertex in the carbon block (Figure 7). In order to increase our sample of events, we did not require perfect events in the spectrometer. We required only that they passed through the dipole magnet and entered the polarimeter. This was done by applying cuts on the proportional chambers before or after the dipole magnet.

Since small angle events had been removed by a hardware processor, all events with $\theta_x < 6^\circ$ were removed from our asymmetry calculation in order to be well away from possible hardware-induced asymmetries. Also, events with $\theta_x > 22^\circ$ were removed. Any instrumental asymmetries that remain are removed by averaging L-R asymmetries for $0^\circ - 180^\circ$ rotations of the polarimeter.

Using the measured analyzing power², A, the polarization is calculated from

$$P = \epsilon / A_{(6^\circ-22^\circ)}$$

where

$$\epsilon = (L-R) / (L+P)_{(6^\circ-22^\circ)}$$

Figure 8 shows the resulting polarizations at the four beam energies.

The left-right asymmetries and polarizations are listed in Table 1.

Notice that all four energies show a significant non-zero, positive polarization of the order of 6% to 10%.

EXPERIMENTAL CHECKS AND VERIFICATIONS

Simultaneously with the proton events we collected a small sample (10%)

of pions of the same momentum and angle. For these events we have also calculated an asymmetry and 'polarization' assuming they were protons. The result is shown in Table 1 and Figure 8. Of course, spin zero particles cannot exhibit polarization and our result is in agreement with this condition, however, the statistical significance is not great.

The up-down asymmetry has also been measured, summing all energies for the inclusive data. This asymmetry also must be zero since a polarization in the scattering plane would violate spin-parity conservation. In fact, we find a result consistent with zero (Table 1).

There is one additional test of our polarization results. We have displayed in Figure 9 the L-R difference as a function of projected scattering angle, θ_x . The rather uniform dependence on θ_x demonstrates that the asymmetry is not due to some abnormal condition at a discrete angle. Furthermore, we can calculate the shape of $L-R(\theta)$ based on measurements of the carbon analyzing power and single track cross-sections from an Argonne polarized beam experiment.³ The result is shown in Figure 9. Clearly, the shape we observe is consistent with that calculated for an incoming polarized proton.

DISCUSSION OF RESULTS

The discovery of substantial polarization in high energy inclusive processes is a surprise. Calculations by Field,⁴ Paige,⁵ Salin,⁶ and others have indicated small polarizations (2-3%) might be expected at low energies. Further, it is to be expected that this polarization would fall off like $1/M^2\sqrt{s}$. General considerations of angular momentum conservations also indicate a $\sin\theta^*$ dependence. (θ^* is the center of mass production

angle.) Figure 10 shows the predicted shape for P_p for the data collected at 100 to 400 GeV beam energies. Note that the absolute value of the curve is at least a factor of 10 greater than any prediction. We are clearly not in agreement with the magnitude or energy dependence of any simple triple regge model.

These proton polarizations may well be related to the large values seen in inclusive Λ polarizations.⁷ The Λ polarizations at 28 and 300 GeV and $P_T = 1.0$ GeV/c indicated in Figure 10 show large values apparently independent of energy. If the proton and Λ polarization are related we may also expect to see an increase in the proton polarization as the transverse momentum P_T increases. In the case of the Λ the polarization increases to ~30% at $P_T = 1.5$ GeV/c.⁷ Additional measurements at FNAL could confirm this P_T dependence and display any dependence on missing mass, target, or beam energy.

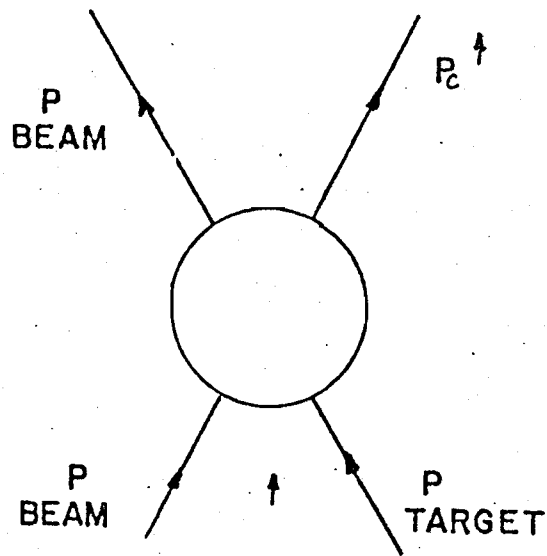
REFERENCES

1. M. D. Corcoran, et al., Preliminary Polarization Results at Fermilab Energies, Indiana University Internal Report IUHEE #9.
2. G. W. Bryant et al., Proton-Carbon Analyzing Power Measurements for Proton Kinetic Energies Between .150 and .440 GeV, Indiana University Internal Report COO-2009-102.
3. R. Koda, Study of $P_{\uparrow}C$ Scattering at 2.0 and 6.0 GeV/c and Possibilities for a Polarimeter, Argonne Internal Report, December 1974.
4. R. D. Field and G. D. Fox, Nucl. Phys. B80, 367 (1974).
5. F. E. Paige and D. P. Sidhu, Phys. Rev. D14, 2307 (1976).
6. P. Salin and J. Soffer, CERN Preprint TH 1769-CERN.
7. G. Bunce et al., Phys. Rev. Let. 36, 1113 (1976).

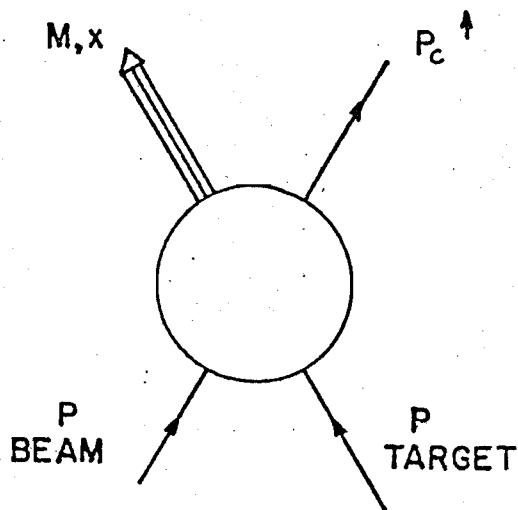
TABLE 1

MEASURED LEFT-RIGHT ASYMMETRY

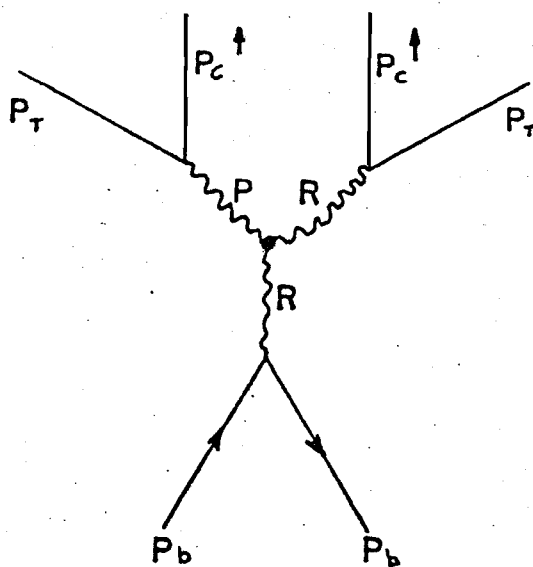
	100 GeV	200 GeV	300 GeV	400 GeV	
Nov. 15, 1976			-.013±.029	.033±.023	180°
			-.017±.021	.016±.020	0°
Feb. 4-5, 1977	.023±.007	.037±.010	.028±.012	.011±.013	180°
	.000±.007	-.004±.009	-.001±.011	.020±.013	0°
Mar. 23, 1977			.015±.013	.034±.018	180°
			.021±.013	-.008±.016	0°
Total	.023±.007	.037±.010	.018±.008	.022±.010	180°
	.000±.007	-.004±.009	.005±.079	.011±.009	0°
Net Asymmetry $\left(\frac{0^\circ+180^\circ}{2}\right)$.011±.005	.016±.007	.011±.006	.016±.007	
Polarization (A=.16)	.066±.030	.095±.040	.067±.034	.095±.003	
Instrumental Asymmetry $\left(\frac{180^\circ-0^\circ}{2}\right)$.011±.005	.020±.007	.007±.006	.006±.006	
Pion asymmetry (energy average)	-.008±.023	-.013±.030	-.010±.025	.005±.031	
Up-down Asymmetry	-.002±.004	180° 0°	.001±.003	$\left(\frac{180^\circ+0^\circ}{2}\right)$	



(a)



(b)



(c)

FIGURE 1

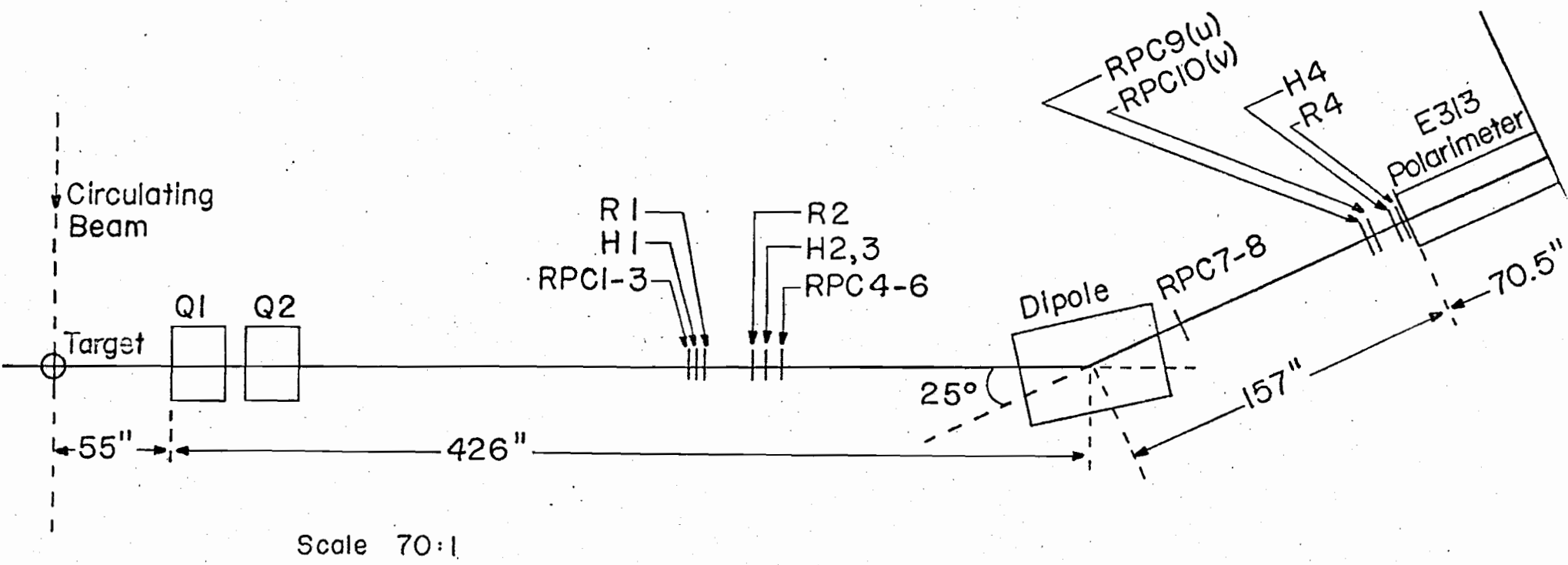
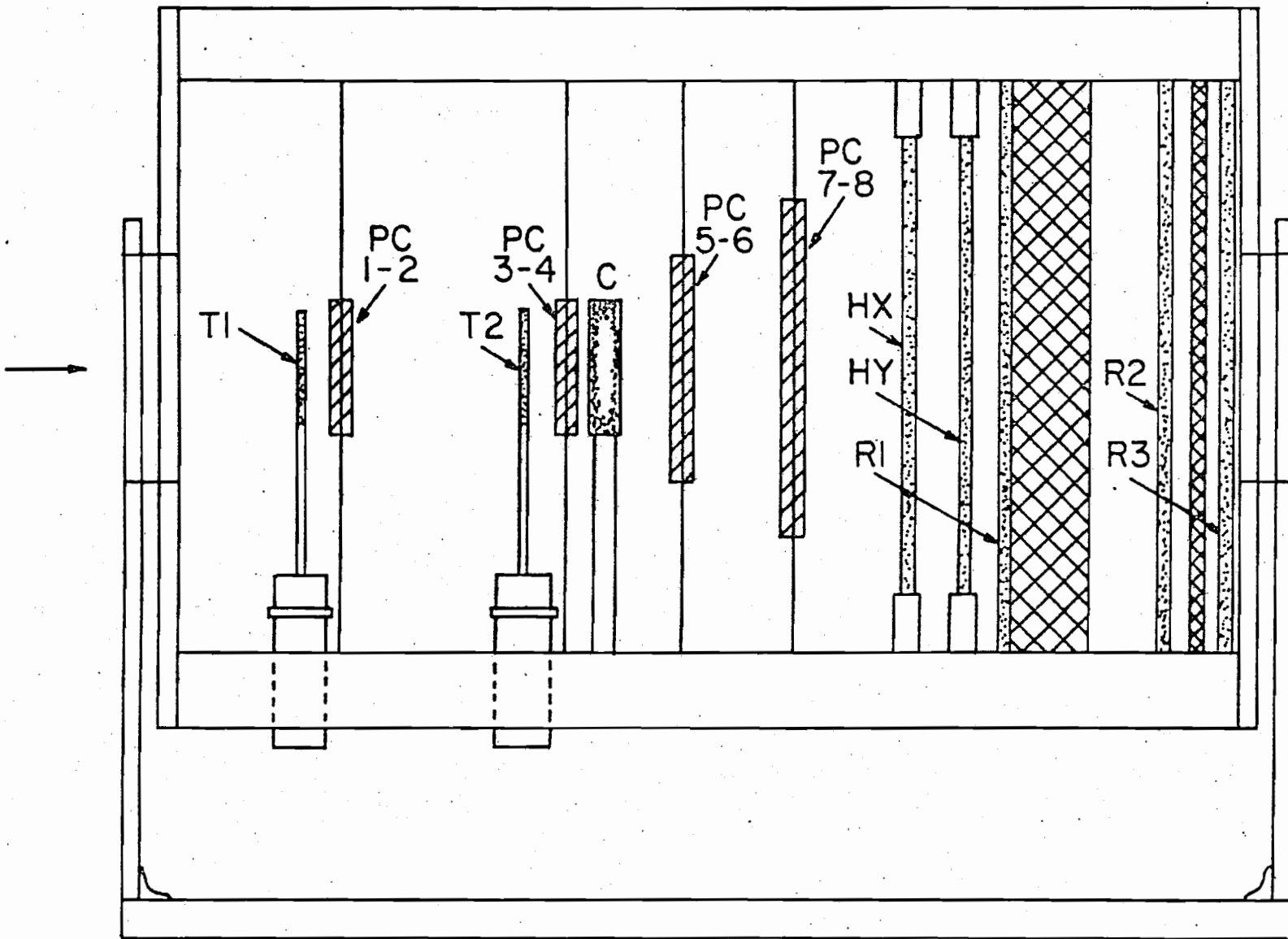





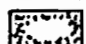
FIGURE 2

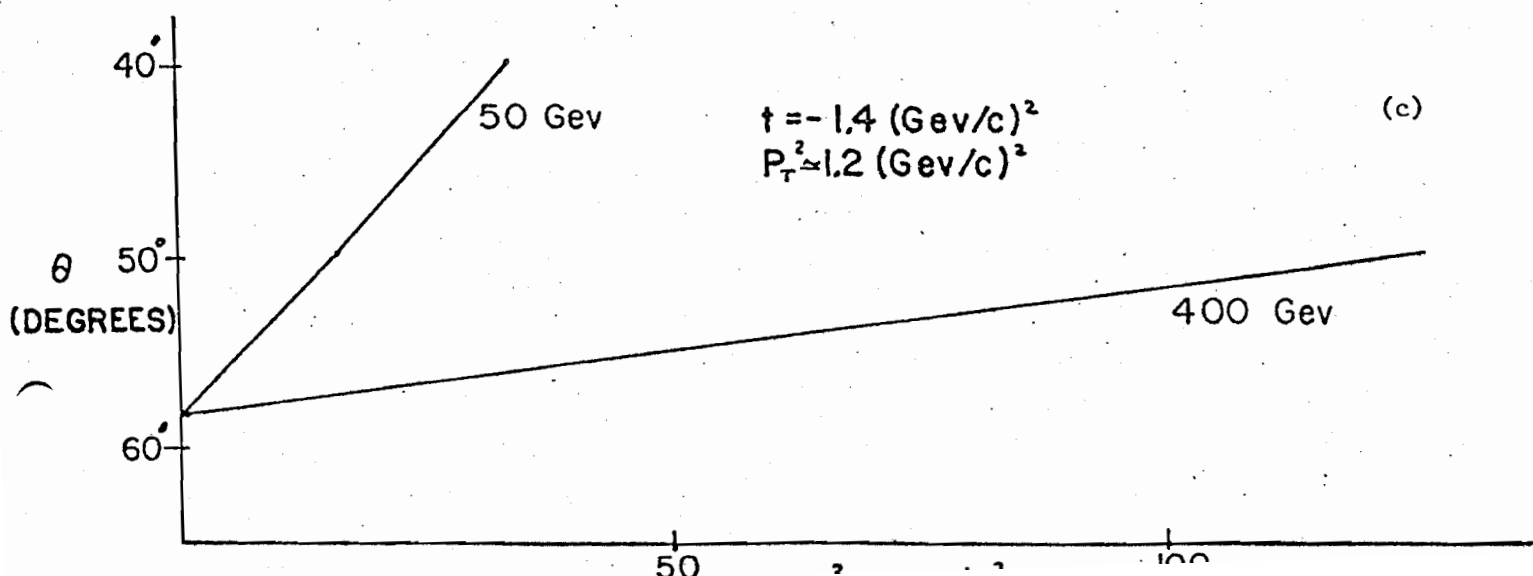
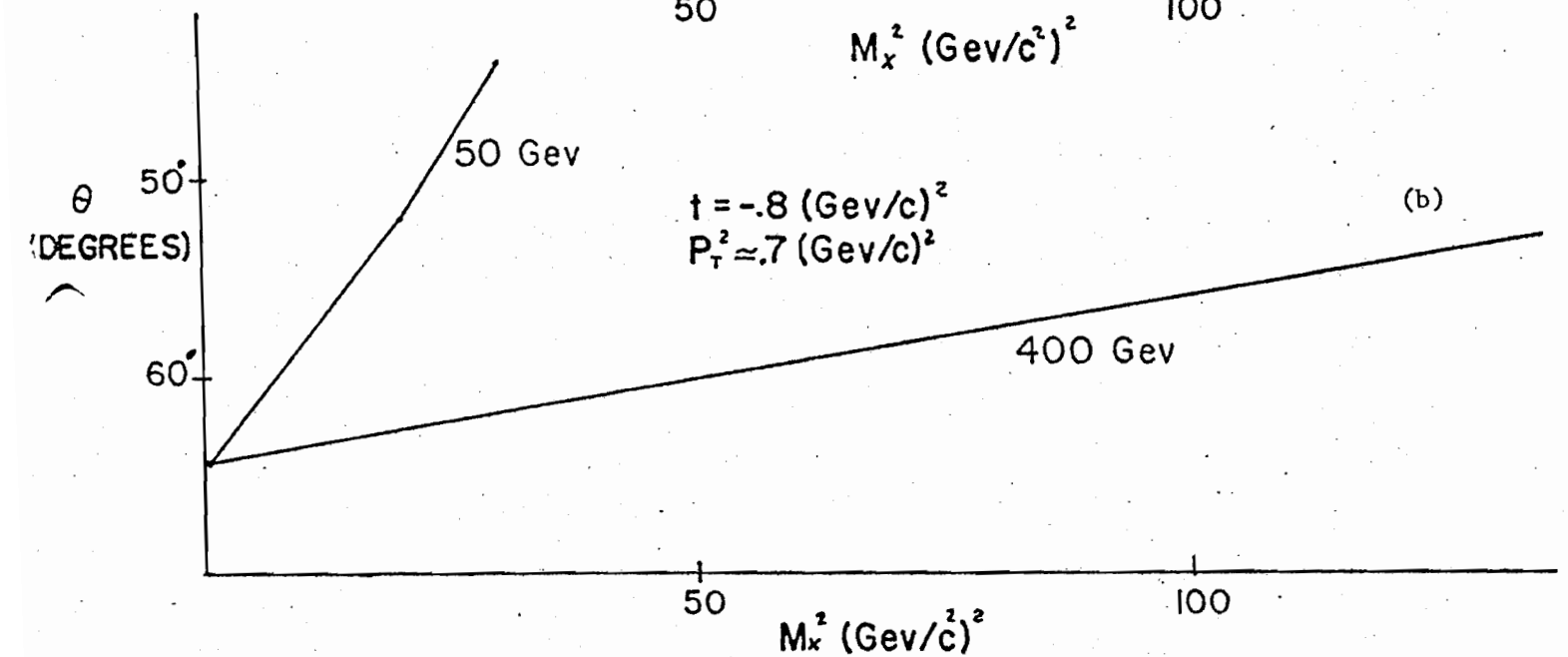
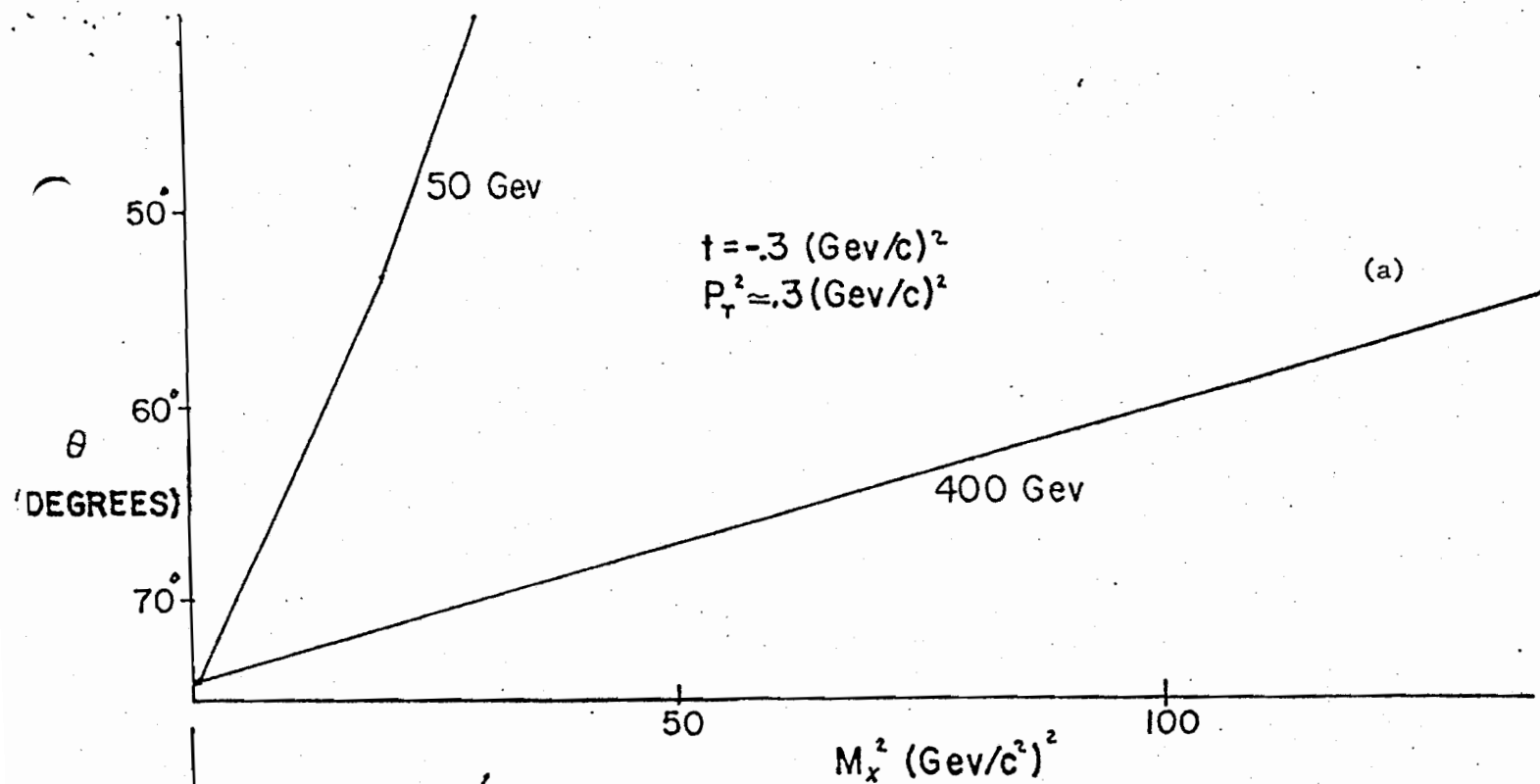
INTERNAL TARGET
SPECTROMETER



POLARIMETER LAYOUT

scale: 8:1

-  proportional chambers
-  range steel
-  scintillation counters
-  carbon block



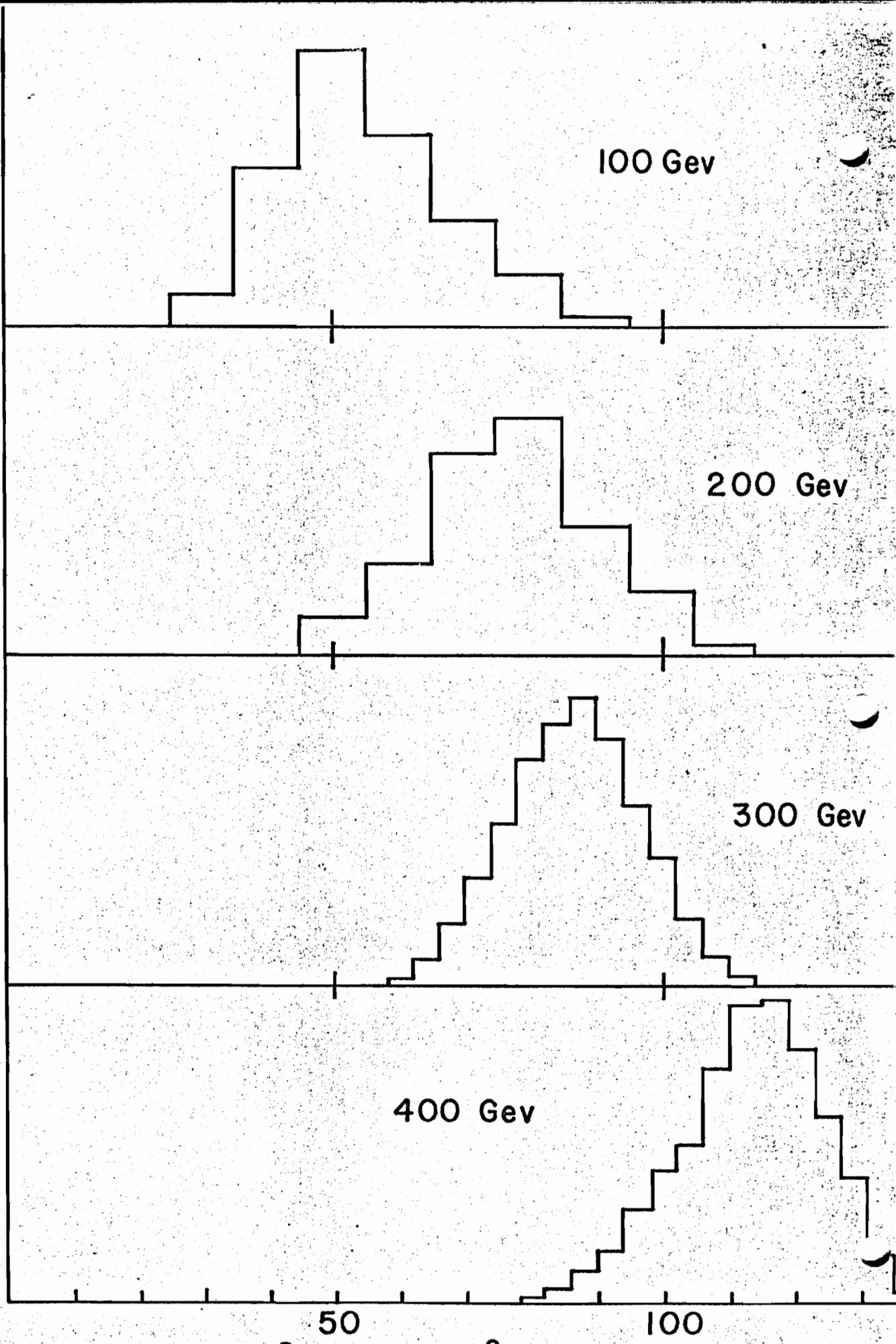


FIGURE 5

Mx^2 (Gev/c²)²

SCATTERING DISTRIBUTION
X-Z PLANE PROJECTION

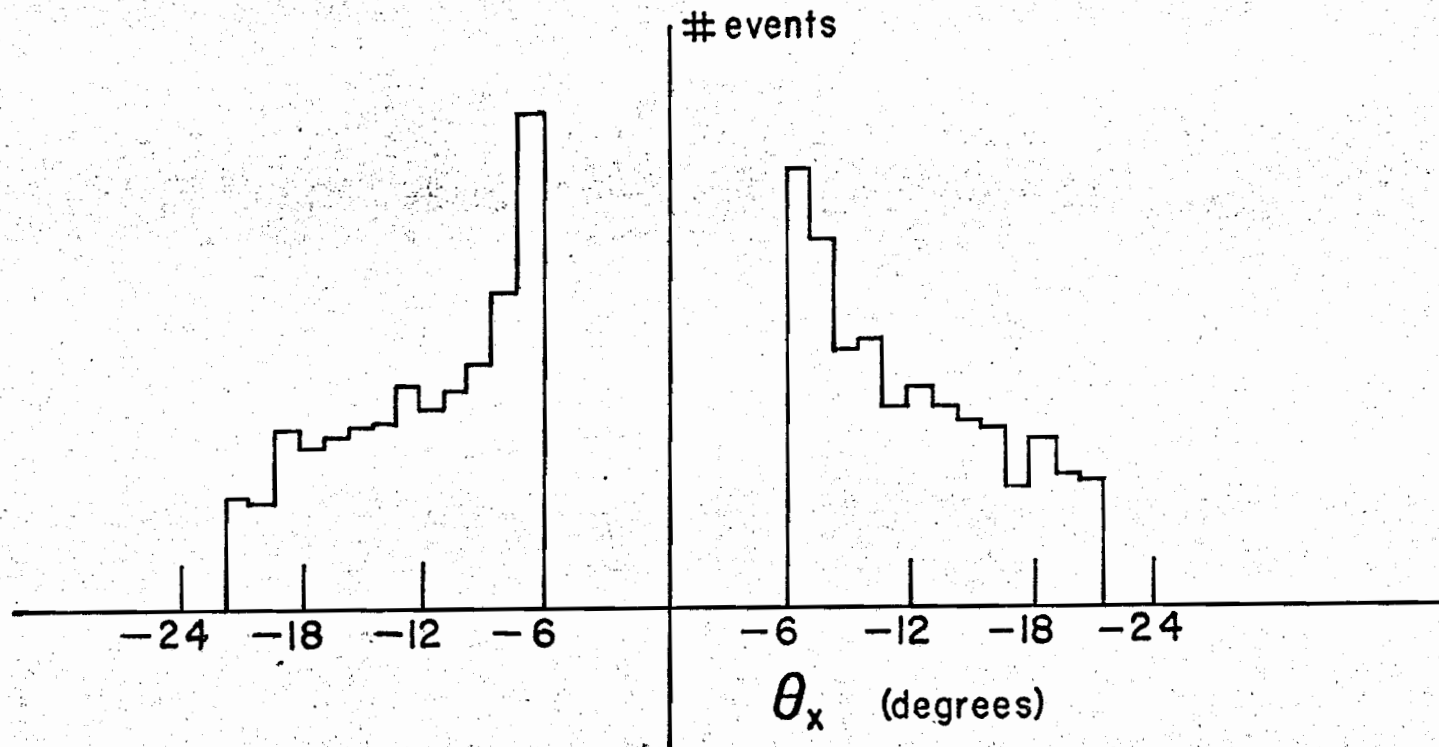


FIGURE 6

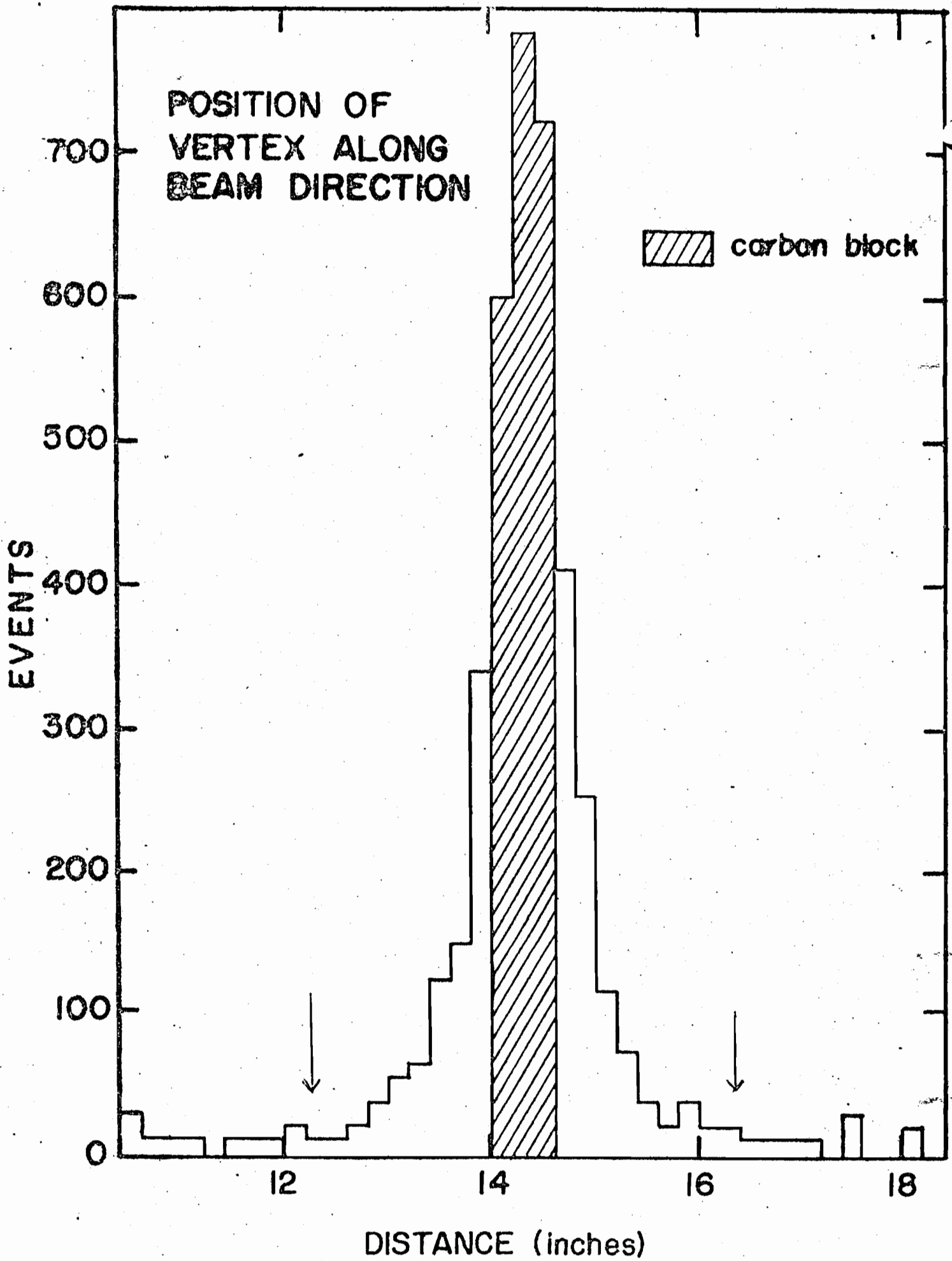


FIGURE 7



$P_T = 1.1 \text{ GeV}/c$
 $x = .88$

(Preliminary)

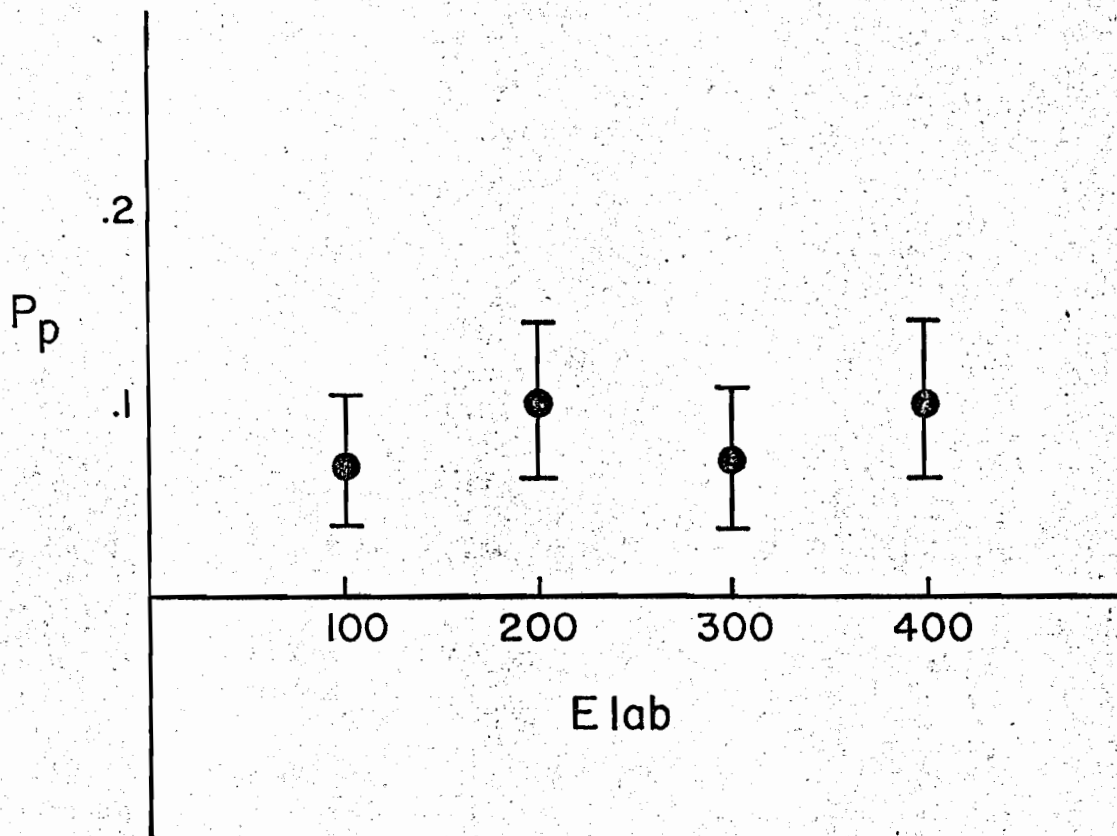


FIGURE 8

(L - R) vs θ

(100, 200, 300, 400 Gev)

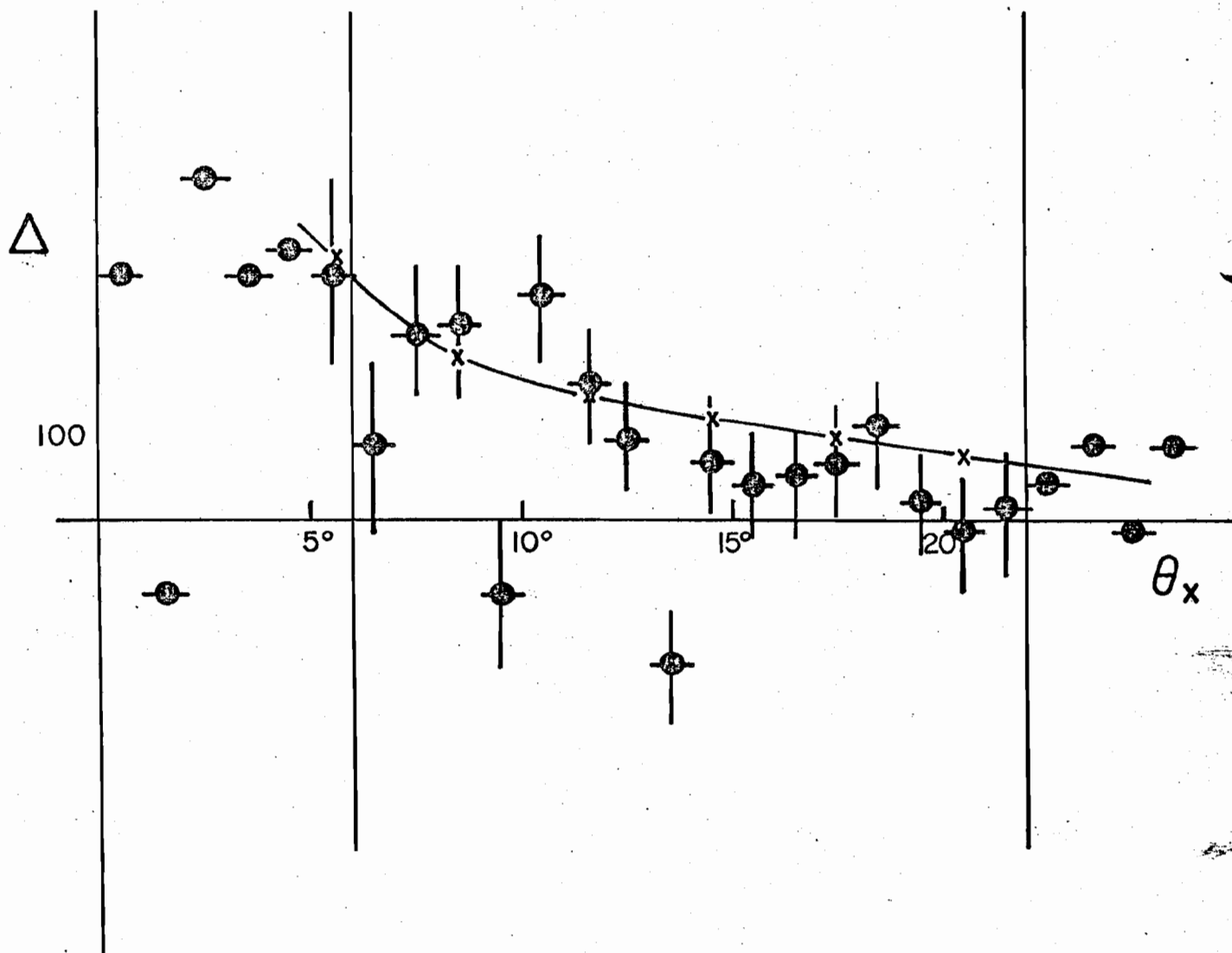
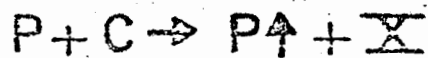


FIGURE 9



$P_T = 1.1 \text{ GeV}/c$

$x = .88$

PRELIMINARY

($\theta = 52^\circ$)

Δ Bunce et al. (Ref. 7)

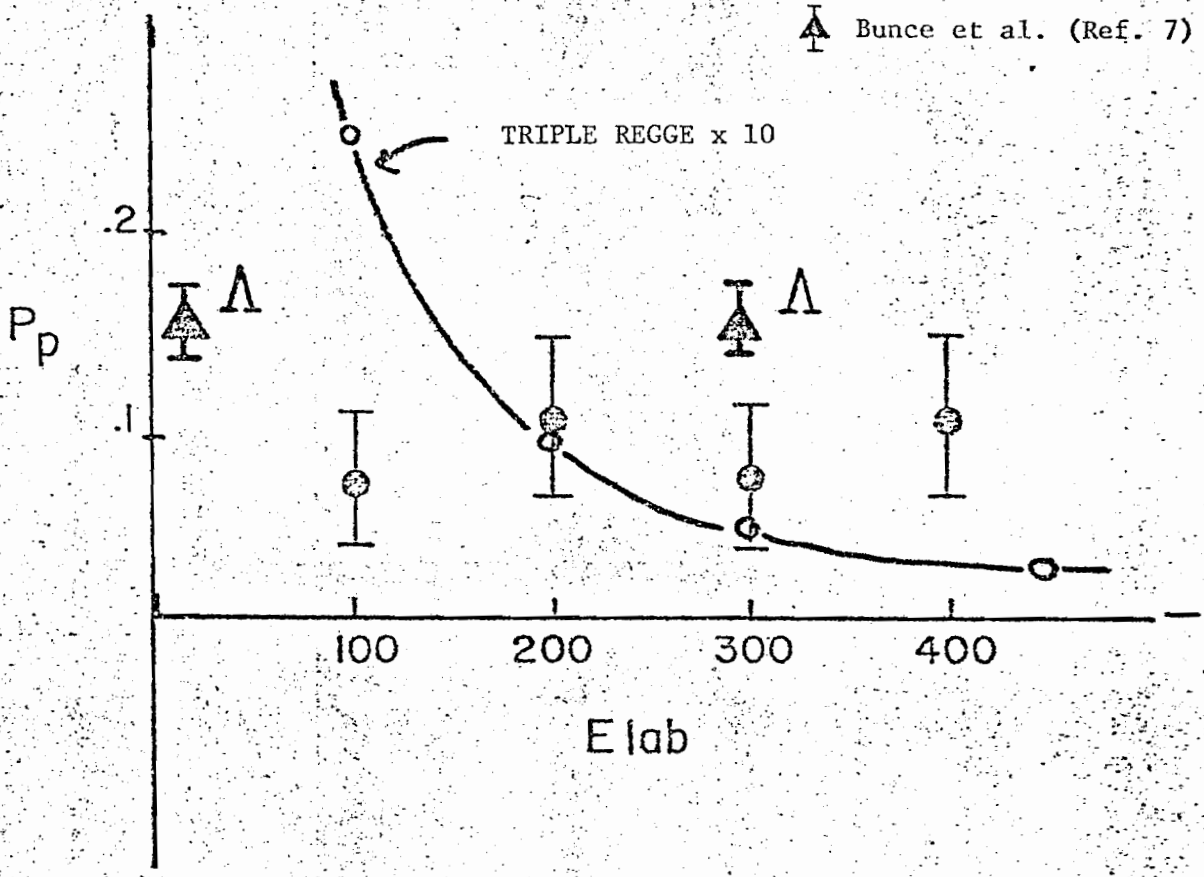


FIGURE 10